# Chemical Science

The chemical science section of this year's NSRRC Activity Report highlights groundbreaking research leveraging synchrotron-based techniques. Studies span diverse fields, including organic photovoltaics, near-infrared (NIR) optoelectronics, photoresponsive materials, catalytic ammonia synthesis, and astrochemistry. These investigations underscore the critical role of synchrotron radiation in elucidating atomic and molecular phenomena, driving scientific and technological advancements.

A pivotal study on nonfullerene acceptors for organic photovoltaics explores the structure–property–performance relationships of a novel acceptor, CB16. By removing the central thiadiazole unit, researchers achieved an 18.32% power conversion efficiency, surpassing the Y6-based counterparts. Small/wide-angle X-ray scattering provided insights into molecular packing and interactions, setting new benchmarks for simplified acceptor designs to enhance the solar cell efficiency.

In NIR optoelectronics, two studies push organic light-emitting diode (OLED) emission wavelengths beyond 900 nm. One exploits an interfacial energy transfer mechanism to achieve hyperfluorescence at 925 nm and 1022 nm using Pt(II) complex and fluorescent dye bilayers, with implications for telecommunications and bioimaging. The other study investigates chromium-doped materials, revealing that luminescence quenching in GaInO<sub>3</sub>:Cr<sup>3+</sup> arises from hole-type thermal quenching rather than electron transfer—a key insight for improving NIR-emitting materials for sensors and LEDs.

A breakthrough in light-responsive materials features MXenegel, a composite hydrogel integrating MXene nanosheets and azobenzene-based supramolecular complexes. Exhibiting reversible phase transitions under UV and visible light without compromising conductivity, this innovation paves the way for reconfigurable soft electronics. Synchrotron techniques were instrumental in probing the gel's structural transformations.

Catalysis remains a focal point, with a study on ammonia synthesis using carbon-supported ruthenium catalysts. Researchers optimized mesoporous carbon supports to enhance catalytic performance and stability, aligning with renewable-energy initiatives. Synchrotron characterizations of Ru nanoparticle dispersion and electronic promoter interactions revealed the mechanisms mitigating hydrogen poisoning, offering scalable solutions for efficient ammonia production.

Astrochemical research explores molecular ices and doped graphene. One study examines the behavior of 1-propanol ice under interstellar conditions, showing its persistence beyond the melting point without crystallization—key for understanding cosmic dust mantles. Another investigates ethanolamine ice, providing insights into its formation pathways and spectroscopic properties, enriching knowledge of prebiotic chemistry in star-forming regions. A final study on N-doped graphene correlates its photoluminescence properties with astrophysical observations of the Red Rectangle Nebula. Synchrotron radiation played a crucial role in characterizing bonding environments and electronic structures.

Collectively, these studies demonstrate the transformative impact of synchrotron-based research. From renewable energy advancements to unraveling cosmic mysteries, NSRRC continues to foster collaborations that push the boundaries of chemical sciences, contributing to sustainable and innovative solutions. (By Yu-Jong Wu)



### **Insights into Molecular Packing**

Controlling  $\pi$ - $\pi$  stacking in non-fullerene acceptors could be key to enhancing organic photovoltaic performance.

rganic photovoltaics (OPVs) have emerged as a promising renewable energy technology due to their lightweight, flexible, and scalable nature, making them ideal for next-generation solar energy solutions. A key factor driving the advancement of OPVs is the development of non-fullerene acceptors (NFAs), which have surpassed fullerene-based acceptors in optical absorption, tunability, and efficiency.1 Among these, Y6-based NFAs stand out as benchmarks, enabling power conversion efficiencies (PCEs) exceeding 18% through their unique A-DA' D-A-type molecular architecture.<sup>2</sup> This structure, featuring a central thiadiazole (Tz) unit and a C-shaped ortho-benzodipyrrole skeleton, supports strong absorption and efficient charge transport. Despite these successes, challenges such as the synthetic complexity of Y6 and its tendency toward aggregation hinder further improvements and limit scalability.

To address these challenges, teams led by Yen-Ju Cheng (National Yang Ming Chiao Tung University) and U-Ser Jeng (NSRRC) are exploring innovative molecular designs aimed at maintaining high performance while minimizing structural complexity and aggregation. This research focused on three carefully designed NFAs—CB16, Y6-16, and SB16—to better understand the relationships between molecular structure, packing behavior, and device performance. As shown in Fig. 1, CB16 simplifies the Y6 architecture by removing the central Tz unit while preserving the C-shaped ortho-benzodipyrrole skeleton.

This modification is intended to reduce self-aggregation and improve donor–acceptor interactions. Y6-16, a derivative of Y6 with side chains identical to those of CB16, retains the Tz unit and serves as a benchmark for comparison. Additionally, SB16 features an S-shaped parabenzodipyrrole skeleton, offering a direct comparison in molecular geometry. These three NFAs were strategically selected to elucidate how structural modifications influence molecular packing, charge transport, and overall device performance.

Grazing-incidence wide-angle X-ray scattering (GIWAXS) and simultaneous small- and wide-angle X-ray scattering (SWAXS) provided detailed insights into the molecular packing and phase behavior of the NFAs in both neat films and when blended with the donor polymer PM6. Figure 2 highlights the GIWAXS patterns and corresponding 1D scattering profiles, revealing the key differences in molecular packing among the three NFAs. CB16 exhibits vertically oriented  $\pi$ – $\pi$  stacking with abundant small nanodomains, facilitating the formation of bicontinuous networks essential for efficient charge transport. This packing arrangement reflects the benefits of removing the Tz unit, which results in reduced aggregation while maintaining robust donor-acceptor interactions. By contrast, SB16 demonstrates large, phase-separated domains with poor  $\pi$ – $\pi$  stacking due to its S-shaped geometry, resulting in suboptimal performance. Y6-16, while similar to CB16 in packing features, shows

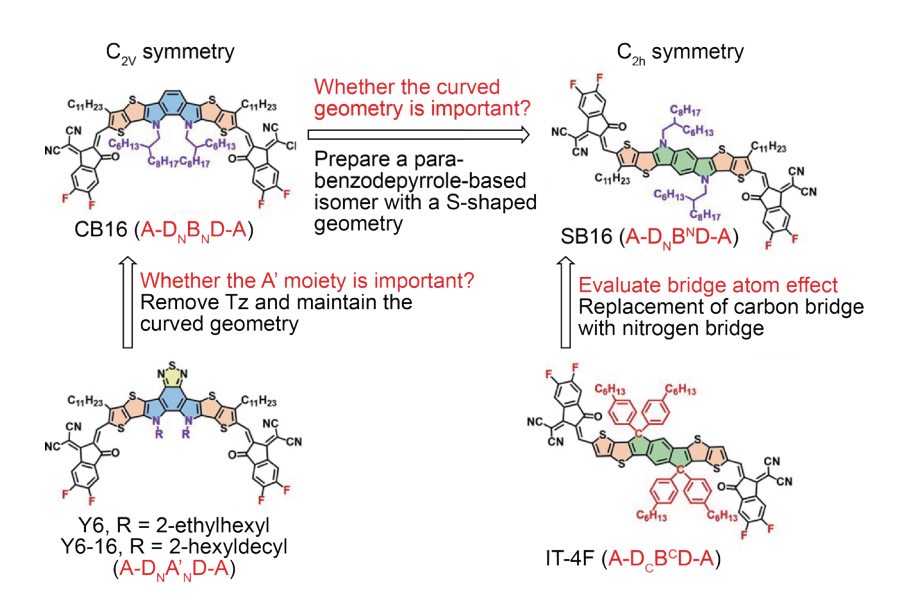


Fig. 1: Chemical structures of Y6, Y6-16, and IT-4F that inspired the design of CB16 and SB16 NFAs. [Reproduced from Ref. 3]

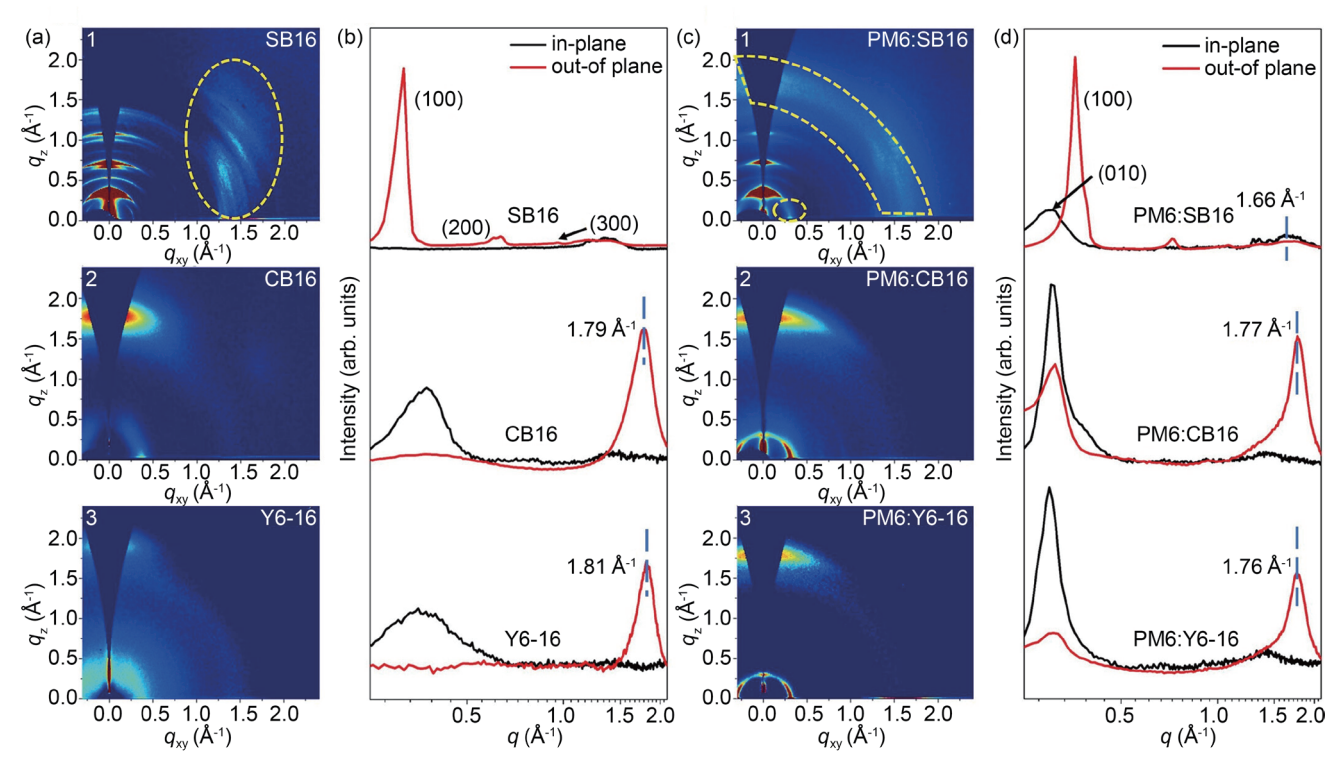


Fig. 2: 2D GIWAXS patterns of the SB16 (a-1), CB16 (a-2), and Y6-16 (a-3) and their blended films PM6:SB16 (c-1), PM6:CB16 (c-2), and PM6:Y6-16 (c-3) and their corresponding 1D scattering profiles along the in-plane and out-of-plane directions for the neat films (b) and blended films (d), respectively. [Reproduced from Ref. 3]

slightly reduced donor–acceptor interactions due to the presence of the Tz unit. In device studies, CB16, when blended with PM6, achieved a remarkable PCE of 18.32% in binary OPV devices, surpassing both those of Y6-16 and SB16. The enhanced performance of CB16 is attributed to its optimized molecular packing, reduced aggregation, and efficient charge transport properties. By removing the Tz unit, CB16 not only simplifies molecular design but also balances structural simplicity with high performance, making it a promising candidate for scalable OPV applications. The contrast in performance between CB16 and SB16 underscores the critical role of molecular geometry, with the C-shaped architecture of CB16 and Y6-16 offering significant advantages over the S-shaped design.

In summary, this study provides insights into the structure–property–performance relationships of NFAs. The C-shaped A-DNBND-A skeleton in CB16 plays a crucial role in promoting efficient  $\pi$ – $\pi$  stacking, reducing aggregation, and enhancing donor–acceptor interactions. The removal of the Tz unit simplifies synthesis while improving phase separation and charge transport, demonstrating the potential for designing high-performance NFAs with reduced complexity. Furthermore, advanced synchrotron-based characterization techniques such as GIWAXS and SWAXS at **TLS 23A1** proved invaluable for revealing the molecular packing behaviors and guiding rational

molecular design. By leveraging rational sample design and state-of-the-art characterization methods, this study not only advances the understanding of NFAs but also paves the way for future innovations in OPVs. The findings emphasize the importance of integrating molecular design, structural analysis, and device optimization to overcome limitations in existing NFAs. (Reported by Hao Ming Chen, National Taiwan University)

This report features the work of Yen-Ju Cheng and U-Ser Jeng published in J. Am. Chem. Soc. **146**, 833 (2024).

#### TLS 23A1 Small/Wide Angle X-ray Scattering

- GIWAXS, GISAXS
- Materials Science, Thin-film Chemistry

- C. Yan, S. Barlow, Z. Wang, H. Yan, A. K. Y. Jen, S. R. Marder, X. Zhan, Nat. Rev. Mater. 3, 18003 (2018).
- G. Zhang, F. R. Lin, F. Qi, T. Heumüller, A. Distler, H.-J. Egelhaaf, N. Li, P. C. Y. Chow, C. J. Brabec, A. K.-Y. Jen, H.-L. Yip, Chem. Rev. 122, 14180 (2022).
- 3. Y.-J. Xue, Z.-Y. Lai, H.-C. Lu, J.-C. Hong, C.-L. Tsai, C.-L. Huang, K.-H. Huang, C.-F. Lu, Y.-Y. Lai, C.-S. Hsu, J.-M. Lin, J.-W. Chang, S.-Y. Chien, G.-H. Lee, U-Ser Jeng, Y.-J. Cheng, J. Am. Chem. Soc. **146**, 833 (2024).

## **Advancing the Frontiers of Near-Infrared Optoelectronics**

Innovative approaches advance NIR emission technologies by improving their quantum efficiency, energy transfer, and thermal stability.

The field of near-infrared (NIR) optoelectronics has emerged as a critical area of innovation driven by the increasing demand for high-performance materials and devices across diverse applications, from bioimaging and sensing to advanced communication systems. Researchers have actively striven to overcome fundamental challenges such as low quantum efficiencies, energy loss, and thermal instability. The development of novel materials and device architectures has emerged as a cornerstone of progress in this domain. This highlight presents two pioneering studies that exemplify the synergy of materials sciences, photophysics, and engineering in advancing NIR technologies.

Traditional organic light-emitting diodes (OLEDs) in the NIR range have faced challenges related to low external quantum efficiencies (EQEs). This issue is caused by the emission energy gap law, which results in significant nonradiative losses as emission wavelengths extend into the infrared spectrum. This limitation often leads to inefficiencies that hinder the practical implementation of NIR OLEDs in fields such as bioimaging, data communication, and advanced sensing. To overcome these barriers, a collaborative research group led by Yun Chi (City University of Hong Kong, China) and Pi-Tai Chou (National Taiwan University) has introduced an innovative bilayer device architecture incorporating Pt(II) complexes and fluorescent dyes such as BTP-eC9. The components of the architecture are engineered to form a synergistic donor-acceptor system. By leveraging interfacial energy-transfer mechanisms, this architecture achieves hyperfluorescence with peak emissions at 925 nm and EQEs of 2.24%, setting a new benchmark in the field. Additionally, the integration of a transfer printing method preserves the integrity of delicate molecular assemblies, ensuring efficient energy transfer and device stability. A grazingincidence wide-angle X-ray scattering (GIWAXS) analysis performed at TLS 13A1 revealed that the Pt(II) complexes in the OLED architecture exhibited highly ordered edge-on  $\pi$ - $\pi$  stacking, which is crucial for efficient energy transfer. The BTP-eC9 fluorescent dye displayed lamellar-type face-on  $\pi$ - $\pi$  stacking, which is also important for its function as an energy acceptor and emitter, facilitating the interfacial energy transfer mechanisms. Thus, the Pt(II) complexes act as highly efficient energy donors, transferring triplet-state energy to the singlet-state acceptors (BTP-eC9) via a Förster resonance energy transfer (FRET) mechanism, as demonstrated in Fig. 1. This process bypasses nonradiative loss channels, enhancing fluorescence intensity. A bilayer architecture with precise control over material interfaces minimizes back energy transfer and maintains structural order. The implementation of transfer printing addresses the challenge of assembling self-organized layers while maintaining their molecular arrangement, demonstrating the potential for large-scale manufacturing. This research not

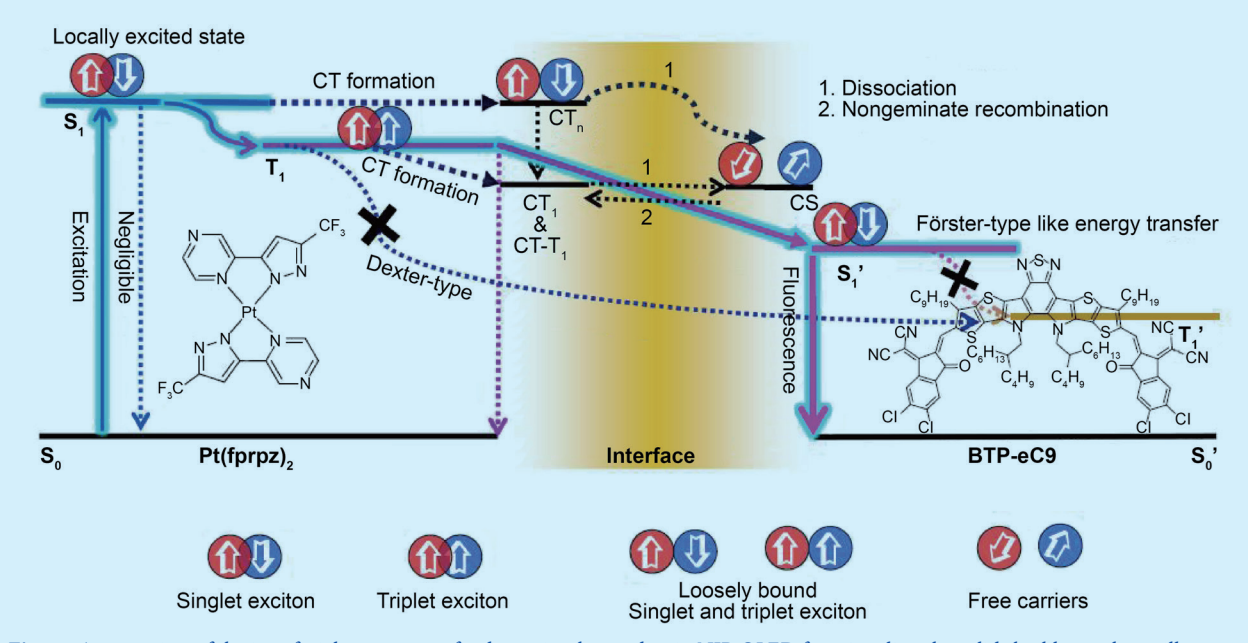


Fig. 1: An overview of the interfacial energy transfer dynamics that underpin NIR OLED functionality: the solid sky-blue pathway illustrates the interfacial energy-transfer process, which facilitates FRET. In this context, the S<sub>0</sub> and S<sub>1</sub> states represent the ground and excited states, respectively, of the singlet manifold, and the T<sub>1</sub> state denotes the triplet state. [Reproduced from Ref. 1]

only demonstrates a leap in device performance but also establishes a robust framework for tackling the inherent limitations imposed by the emission energy gap law.

The second significant research contribution comes from Sebastian Mahlik of the University of Gdansk, Poland, focusing on inorganic materials, specifically, Ga-In oxides doped with Cr3+ ions.2 This study investigates the dual-purpose functionality of these materials as NIR phosphors for light-emitting diodes (LEDs) and ultraviolet photodetectors. The research examines the intricate interplay between radiative and nonradiative processes, emphasizing luminescence-quenching mechanisms. Cr³+-activated materials have attracted significant attention for their ability to emit broadband NIR light, positioning them as ideal candidates for phosphor-converted LEDs. However, traditional interpretations of luminescence quenching often fail to explain the unique thermal behaviors observed in these systems. This study presents a novel perspective by attributing luminescence quenching to hole-based thermal ionization rather than electron transfer to the conduction band—a paradigm shift in understanding transition-metal-doped luminescent materials. High-resolution synchrotron X-ray diffraction (XRD) data, obtained at TPS 19A, revealed that Ga-In oxide samples predominantly exhibit a monoclinic β-Ga<sub>2</sub>O<sub>3</sub> structure. Increasing indium ( $In^{3+}$ ) doping levels led to the coexistence of two phases: the monoclinic  $\beta$ -Ga<sub>2</sub>O<sub>3</sub> phase and the cubic In<sub>2</sub>O<sub>3</sub> phase. This phase separation underscores the limited solubility of In<sup>3+</sup> in the Ga<sub>2</sub>O<sub>3</sub> host lattice and the structural changes induced by In3+ substitution. Greater indium concentrations introduced more disorder into the crystal lattice, as evidenced by the broadening of peaks in diffraction patterns and the appearance of mixed phases at higher doping levels. This disorder affected the local crystal field around Cr<sup>3+</sup> dopants, significantly influencing their optical and photoelectric properties.

The study presents a groundbreaking hole-based thermal quenching mechanism, which challenges the conventional focus on electron transfer. This mechanism accounts for the material's luminescence behavior at elevated temperatures. The  $Ga_{1\cdot 98\cdot x}In_xO_3:0.02Cr^{3+}$  system exhibits tunable NIR emission and efficient photocurrent generation, rendering it suitable for both light emission and detection applications. By combining high-resolution synchrotron XRD with photoluminescence analysis, the research links In-induced structural modifications to enhanced optical performance. The substitution of  $In^{3+}$  ions alters the crystal field environment, optimizing energy level alignments for NIR emission and expanding the material's functionality in optoelectronic applications.

Together, these studies provide a comprehensive exploration of the challenges and solutions shaping the future of NIR optoelectronics. The meticulous research on OLEDs emphasizes the importance of molecular precision and device architecture, whereas the insights into Cr³+-activated materials highlight the interplay between structure, energy dynamics, and multifunctionality. By connecting organic and inorganic systems, this compilation highlights the shared principles that underpin success in the field: innovation in material design, rigorous characterization, and a vision for translational impact. (Reported by Yu-Jong Wu)

This report features the work of Yun Chi, Pi-Tai Chou and their collaborators published in Nat. Commun. **15**, 4664 (2024), and the work of Sebastian Mahlik and his collaborators published in JACS **146**, 22807 (2024).

# TPS 19A High-resolution Powder X-ray Diffraction TLS 13A1 X-ray Scattering

- GIWAXS, XRD
- Materials Science, Inorganic Chemistry, Solid-state Chemistry, Photoluminescence

- 1. C.-M. Hung, S.-F. Wang, W.-C. Chao, J.-L. Li, B.-H. Chen, C.-H. Lu, K.-Y. Tu, S.-D. Yang, W.-Y. Hung, Y. Chi, P.-T. Chou, Nat. Commun. 15, 4664 (2024).
- 2. N. Majewska, M.-H. Fang, Sebastian Mahlik, JACS 146, 22807 (2024).

## **Light-Activated Gel: Paving the Way for Smarter Electronics**

A novel light-responsive gel combining MXene nanosheets with supramolecular complexes was investigated, showcasing reversible phase transitions and enhanced conductivity.

Xenes are a rapidly emerging Class of two-dimensional (2D) materials that have garnered significant attention in materials science due to their unique properties and broad applications. First discovered in 2011, MXenes are synthesized by selectively etching out elements from layered transition metal carbides, nitrides, or carbonitrides. MXenes exhibit a unique combination of metallic conductivity, excellent mechanical flexibility, high surface area, and tunable surface chemistry. These attributes make them highly promising for various applications, including energy storage, electromagnetic interference, water purification, and catalysis. The research team led by Jiun-Tai Chen from National Yang Ming Chiao Tung University explored conductive composite gels with multifunctional capabilities. By incorporating inorganic dopants into an organic matrix, the gel's conductivity can be significantly improved while introducing new properties such

as thermal responsiveness, light responsiveness, and self-healing abilities.

The research team studied a lightresponsive MXene-based composite gel, termed MXenegel, which integrates azobenzene-containing supramolecular complexes with MXene nanosheets (**Fig. 1**). This innovative material exhibits reversible photo-modulated phase behavior, transitioning between liquid and solid states under UV and visible light, respectively, while maintaining its electrical conductivity, making it suitable for traditional solid-state electronics. The motivation behind this research stems from the need for intelligent and eco-friendly electronic components that can adapt to environmental changes and promote sustainability. Traditional solid-state materials often lack compatibility with dynamic substrates, such as human skin, and do not respond to environmental stimuli. The MXenegel addresses these challenges

by providing a new charge transport pathway that can sense environmental changes and be reprogrammed or recycled.

Multiple instruments were used in this work, providing spectroscopical and electronic evidence to support the unique behavior of MXenegel. The MXenegel was shown to undergo a gel-to-sol transition upon UV light irradiation, which is attributed to the disassembly of the AzoC6@2αCD inclusions intercalated between the MXene layers. This phase transition is reversible, as the sol-state MXenegel can be converted back to a gel-like structure under visible light irradiation or by keeping it in a dark room at room temperature. Additionally, the X-ray diffraction spectra performed at TLS 23A1 of the NSRRC played an important role in this research. The small-angle X-ray scattering (SAXS) spectra revealed the microstructural details of MXenegel, confirming the successful formation of the AzoC6@2αCD inclusion complexes and their intercalation between MXene layers (Fig. 2).

In summary, this work shows a light-modulated MXenegel with reversible phase transition based on photoresponsive host-guest chemistry. Detailed NMR, 2D-ROESY, XPS, and X-ray scattering analyses obtained from synchrotron facilities revealed the microstructure of the MXenegel. The potential applications of MXenegel in electronic circuitry are diverse and promising. The material could serve as a light-responsive wire in electronic circuits, enabling its integration into solid-state electronics

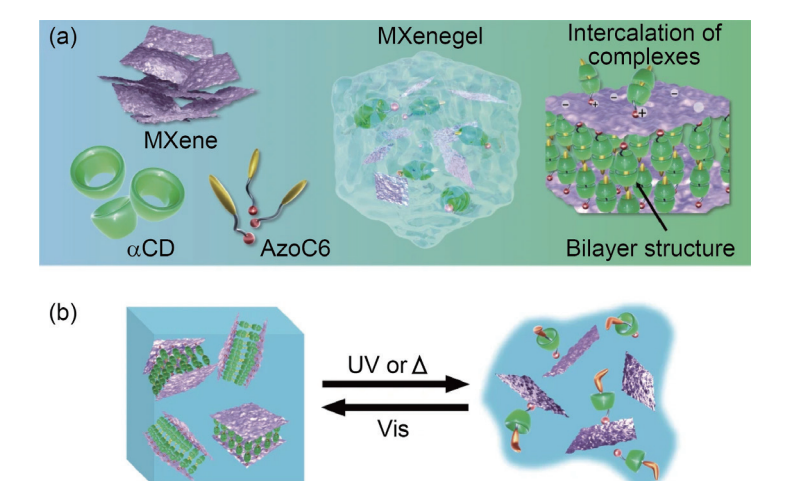


Fig. 1: Schematic illustration of the light-responsive MXenegel. (a) αCD and AzoC6 form a bilayer structure of AzoC6@2αCD supramolecular complexes in MXenes. The positive head ends of the complexes are electrostatically attached to the negatively charged MXene surfaces. (b) Light-responsive sol-gel transition behavior of the MXenegel. [Reproduced from Ref. 1]

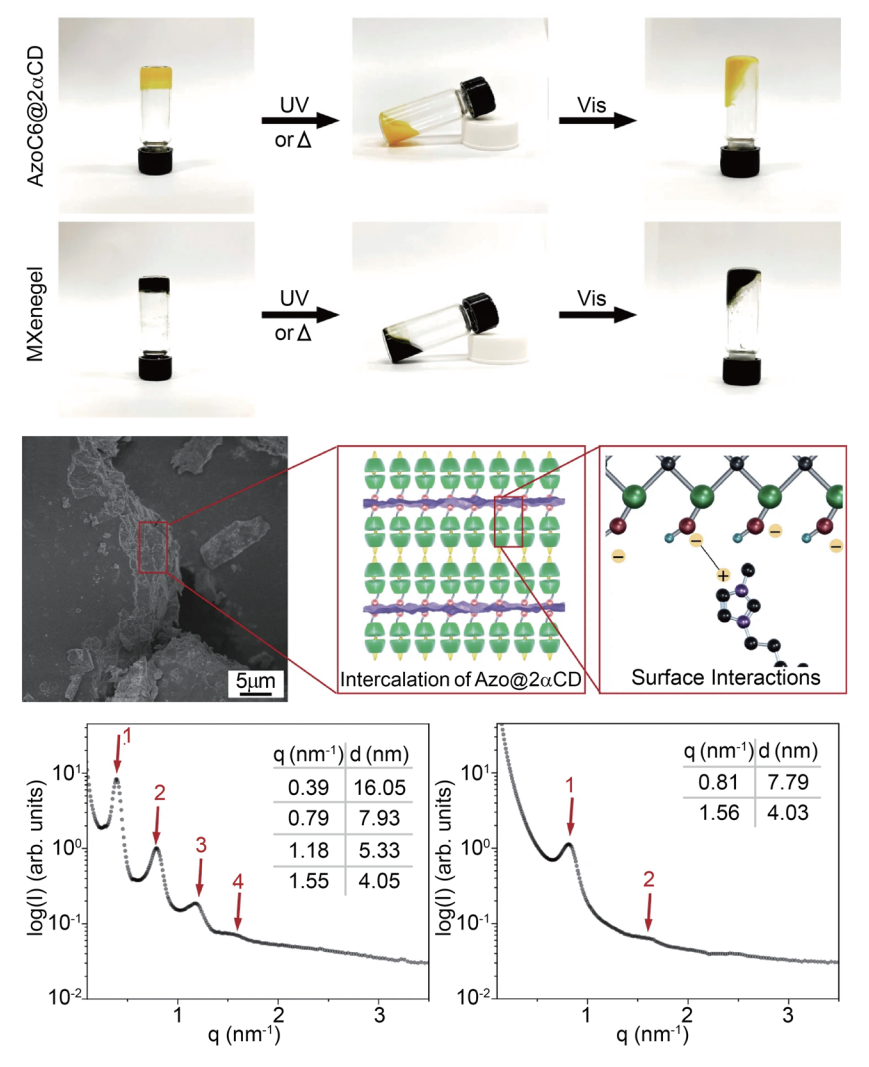


Fig. 2: Light-responsive phase behavior of AzoC6@2αCD and 30 wt% MXenegel under different light irradiations. SEM images of the vacuum-dried MXenegel, in which a cross-sectional view of the MXenegel layers is displayed. The maxima are indicated in the SAXS spectra of AzoC6@2αCD hydrogel and MXenegel. [Reproduced from Ref. 1]

as conductive wires or switches. This material demonstrates a reversible photo-modulated phase behavior, allowing it to function as a photo-controllable switch, which can be utilized to control devices like LEDs. Additionally, MXenegel can be used as a writable and reconfigurable conductive ink, making it suitable for brush printing on various substrates, thus expanding its application in flexible and eco-friendly electronics. (Reported by Yu-Liang Lin, National Yang Ming Chiao Tung University)

This report features the work of Jiun-Tai Chen and his collaborators published in Nat. Commun. **15**, 916 (2024).

# TLS 23A1 Small/Wide Angle X-ray Scattering

- Supramolecular Complex Scattering
- Materials Science, Chemistry, Surface, Thin-film Technology, Chemical Kinetics

#### Reference

 Y.-L. Lin, S. Zheng, C.-C. Chang, L.-R. Lee, J.-T. Chen, Nat. Commun. 15, 916 (2024).

#### **Versatile Roles of Cesium**

Cs-promoted Ru catalysts play a key role in enhancing efficient ammonia synthesis.

Ammonia synthesis is a cornerstone of the global chemical industry as it is essential for fertilizer production and is increasingly recognized as a potential hydrogen carrier for renewable energy applications.¹ However, the conventional Haber–Bosch (HB) process requires high temperatures and pressures, leading to substantial carbon emissions and energy consumption.² In the pursuit of more sustainable and energy-efficient catalytic systems, research teams led by Shih-Yuan Chen (National Institute of Advanced Industrial Science and Technology, Japan), Hsin-Yi Tiffany Chen (National Tsing Hua University), Ho-Hsiu Chou (National Tsing Hua University), and Chia-Min Yang (National Tsing Hua University) investigate the impact of carbon support graphitization on the activity and stability of cesium (Cs)-promoted ruthenium (Ru) catalysts for ammonia synthesis. By systematically tuning the graphitization degree of mesoporous carbon plates (MCPs), this study provides fundamental insights into the relationship between carbon support structure, Ru dispersion, and catalytic performance.

The research introduces a series of Ru catalysts supported on MCPs with varying degrees of graphitization, synthesized through controlled carbonization. MCP-1100, which possesses the highest degree of graphitization, emerges as the optimal support, offering superior thermal stability, enhanced electron conductivity, and minimized carbon methanation. **Figure 1(a)** illustrates that higher carbonization temperatures lead to increased graphitic ordering, further validated by high-angle annular dark-field scanning transmission electron microscopy images. These images reveal well-dispersed Ru nanoparticles on MCP-1100 (**Fig. 1(b)**). By contrast, catalysts supported on lower-graphitization-degree MCPs exhibit Ru particle agglomeration, which negatively impacts catalytic efficiency. The catalytic performance evaluation, presented in **Fig. 1(c)**, demonstrates that the Cs-promoted Ru/MCP-1100 catalyst achieves an ammonia synthesis rate of 43 mmol NH<sub>3</sub>·g<sup>-1</sup>·h<sup>-1</sup> at 410 °C under ambient pressure, significantly outperforming conventional Fe-based catalysts under the similar conditions. These results indicate a strong correlation between the degree of graphitization and ammonia synthesis rates, with higher graphitization promoting better Ru dispersion and electronic conductivity. The critical role of cesium promotion is further supported by density functional theory (DFT) calculations (**Fig. 1(d)**), which show that CsOH weakens hydrogen adsorption on Ru, facilitating ammonia formation by accelerating hydrogen desorption. This cooperative effect between Ru and Cs enhances catalytic efficiency by promoting the crucial dissociative adsorption of N<sub>2</sub> while preventing catalyst deactivation.

A major highlight of this study is the application of *in situ* X-ray absorption spectroscopy (XAS) at **TLS 01C1** for the Ru K-edge and **TLS 17C1** for the Cs  $L_3$ -edge, along with near-ambient-pressure X-ray photoelectron spectroscopy (NAP-XPS) at **TLS 24A1**. These techniques provide real-time insights into the electronic and structural evolution of Ru and Cs species

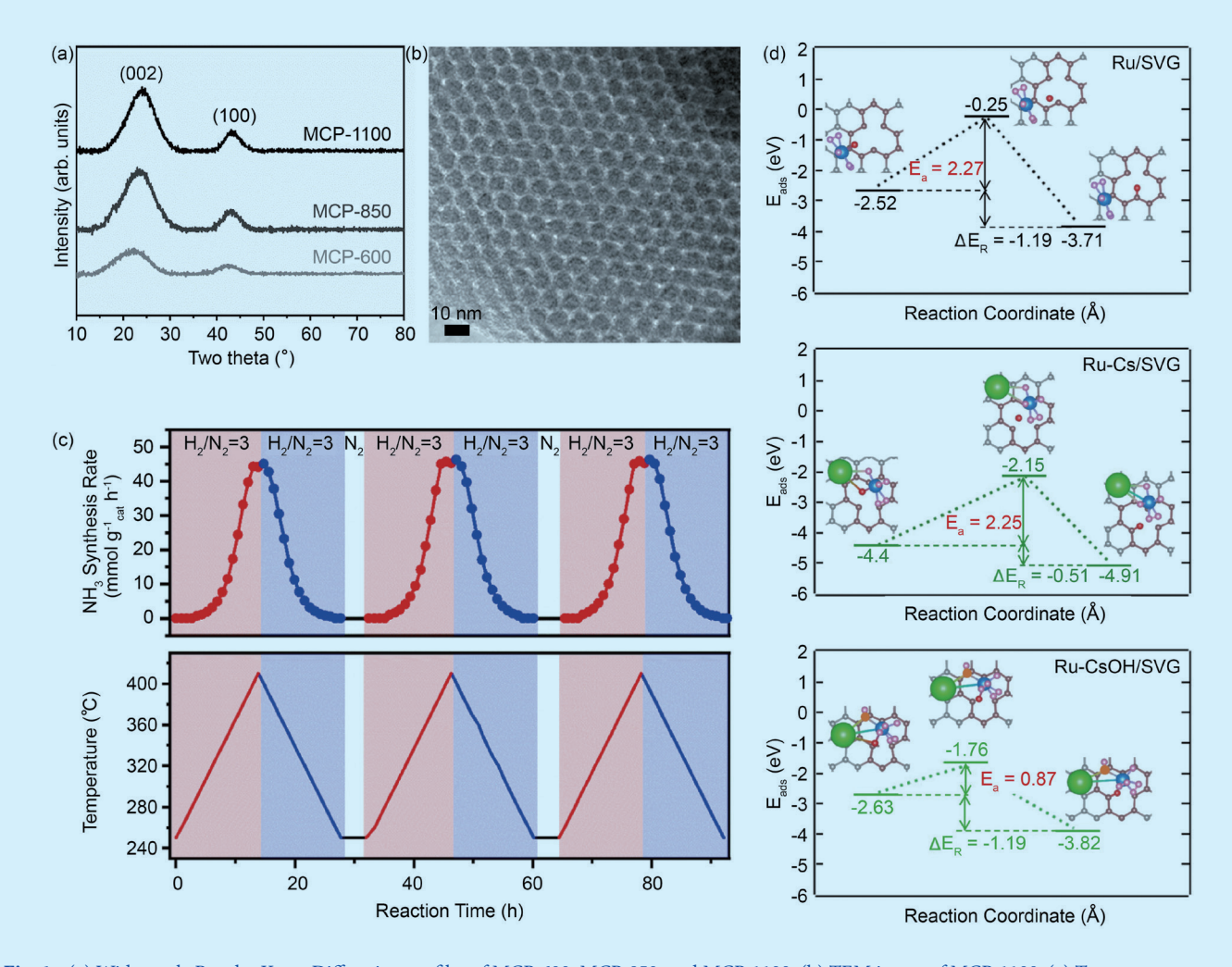


Fig. 1: (a) Wide-angle Powder X-ray Diffraction profiles of MCP-600, MCP-850, and MCP-1100. (b) TEM image of MCP-1100. (c) Temperature dependence of ammonia synthesis rate over 2.5Cs-10Ru/MCP-1100 under intermittent operating conditions. (d) Reaction coordinate diagram of hydrogen spillover from a Ru atom to single-vacancy graphene (SVG) in Ru/SVG, Ru–Cs/SVG, and Ru–CsOH/SVG models with hydrogen saturated at a Ru/H ratio of 1:6. Ea refers to the activation energy for hydrogen spillover from non-spillover models to spillover models through transition states (structures shown on the left, right, and middle in each image, respectively). ΔE<sub>R</sub> refers to the reaction energy between non-spillover and spillover models. Blue, Ru; pink, H; red, spilled-over H; green, Cs; orange, O; gray, C atom away from the C point defect; brown, C atom close to the C point defect. [Reproduced from Ref. 3]

under various reaction conditions. **Figure 2** presents *in situ* X-ray absorption near-edge structure (XANES) and NAP-XPS spectra, which reveal a dynamic transformation of cesium species from CsOH to metallic Cs $^{0}$  during the reaction. This transformation, facilitated by hydrogen spillover from Ru sites, enhances the electron-donating ability of Ru, reducing hydrogen poisoning and increasing N<sub>2</sub> activation. The XAS and NAP-XPS results confirm that Cs $^{0}$  acts as an electronic promoter, effectively modifying the electronic structure of Ru to boost NH $_{3}$  synthesis rates.

In summary, this study establishes that Ru nanoparticle size, Cs/Ru ratio, and the degree of graphitization critically influence NH<sub>3</sub> synthesis rates and resistance to carbon methanation. By leveraging *in situ* XAS, NAP-XPS, kinetic analyses, and theoretical modeling, this work provides a real-time mechanistic understanding of how Cr species dynamically enhance Ru's catalytic performance. The findings establish a new design paradigm for next-generation ammonia synthesis catalysts, offering a scalable and energy-efficient alternative to conventional HB catalysts while mitigating carbon emissions. These insights contribute to the ongoing transition toward sustainable and low-carbon chemical manufacturing. (Reported by Hao Ming Chen, National Taiwan University)

This report features the work of Chia-Min Yang, Ho-Hsiu Chou, Hsin-Yi Tiffany Chen and Shih-Yuan Chen published in Appl. Catal. B-Environ. **346**, 123725 (2024).

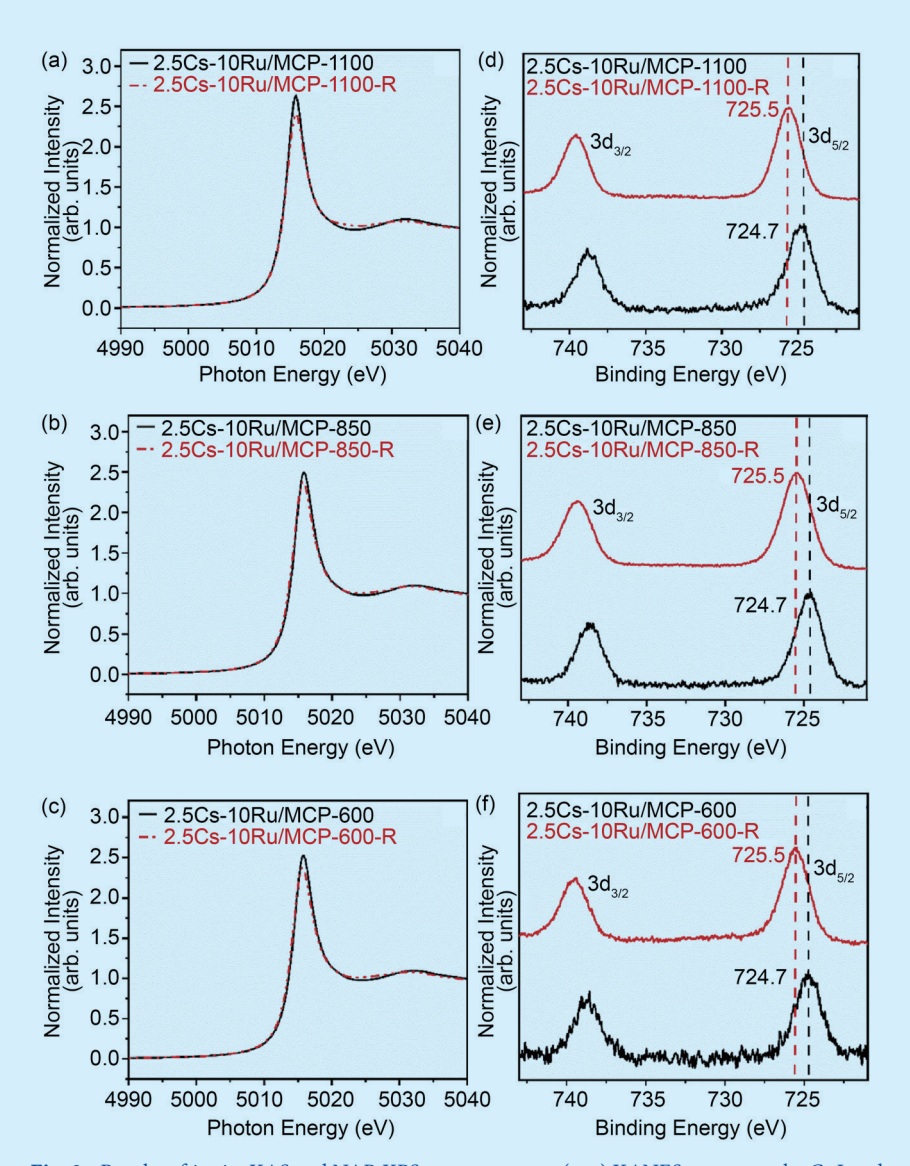


Fig. 2: Results of in situ XAS and NAP-XPS measurements. (a–c) XANES spectra at the Cs  $L_3$ -edge, and (d–f) NAP-XPS profiles of the Cs 3d region. [Reproduced from Ref. 3]

# TLS 01C1 EXAFS TLS 17C1 EXAFS TLS 24A1 XPS, UPS, XAS, APXPS

- In situ XAS, NAP-XPS
- Materials Science, Ammonia Synthesis

- S. Giddey, S. P. S. Badwal, C. Munnings, M. Dolan, ACS Sustain. Chem. Eng. 5, 10231 (2017).
- F. Schüth, R. Palkovits, R. Schlögl,
   D. S. Su, Energy Environ. Sci. 5,
   6278 (2012).
- 3. S.-Y. Chen, L.-Y. Wang, K.-C. Chen, C.-H. Yeh, W.-C. Hsiao, H.-Y. Chen, M. Nishi, M. Keller, C.-L. Chang, C.-N. Liao, T. Mochizuki, H.-Y. T. Chen, H.-H. Chou, C.-M. Yang, Appl. Catal. B-Environ. 346, 123725 (2024).

# Illuminating the Cosmic Laboratory with Vacuum Ultraviolet Light

Exploring the origin and evolution of interstellar and circumstellar molecules enhances our understanding of the Universe.

In the vast expanse of the cosmos, scientists are continuously uncovering secrets that bridge the gap between stars and the building blocks of life. Among these pursuits, three recent studies used the vacuum ultraviolet (VUV) beamlines of the Taiwan Light Source (TLS) to illuminate intriguing connections between interstellar chemistry, materials science, and the potential origins of life. These stories unfold like chapters in a grand cosmic narrative, each offering a glimpse into the intricate dance of molecules and light in the universe.

The first story begins with ethanolamine, a simple molecule with profound implications. Known as a precursor to amino acids, ethanolamine has the potential to unveil how the building blocks of life might have formed in the harsh environments of space. A joint research group led by Bhalamurugan Sivaraman from Physical Research Laboratory of India, delved into its mysteries by recreating astrochemical conditions in the laboratory. Using advanced spectroscopy, they probed the spectral fingerprints of this molecule, capturing the behavior of ethanolamine ice as it is warmed from frigid interstellar temperatures.1 Infrared and VUV spectroscopy provided critical insights, revealing how the molecule interacts with ultraviolet photons and sublimates as it transitions to higher temperatures. The end station connected to TLS 03A1 employed ultrahigh vacuum chambers to mimic interstellar conditions, with ethanolamine deposited on cryogenically cooled substrates. These setups allowed for precise control of temperature and environment, ensuring that the behavior of the molecule could be observed without interference. Coupled with computational models, this work pieced together plausible pathways for the molecule's formation on cosmic dust grains, providing a roadmap for future discoveries of prebiotic chemistry in the cosmos.

Next, their focus shifted to 1-propanol, a fatty alcohol that holds the potential to shed light on the origins of proto-cell membranes. The tale of 1-propanol is one of resilience, as experiments revealed its unusual stability in the icy realms of the interstellar medium. Despite warming beyond its melting point, this molecule defied expectations, remaining amorphous and adhering to simulated dust grain surfaces.<sup>2</sup> Mid-infrared spectroscopy was again employed to trace the molecular vibrations of 1-propanol across a range of temperatures, while VUV spectroscopy captured its absorption characteristics in the 115–220 nm range, as shown in **Fig.1**. Using a cryostat system with

LiF windows and controlled heating rates, researchers meticulously documented the phase transitions and sublimation behavior of 1-propanol. The VUV spectra of 1-propanol were recorded well beyond its melting point of 147 K, demonstrating that the solid-state sample remained amorphous throughout the warming process, from 10 K to 175 K, until sublimation. This represents the first observation of a molecule persisting on a cold substrate beyond its melting point in a UHV chamber. In contrast, 2-propanol, a positional isomer of 1-propanol, exhibits entirely different behavior: it crystallizes at approximately 120 K and sublimates at 150–155 K, prior to reaching its melting point. Mid-infrared spectroscopy was again employed to trace the molecular vibrations of 1-propanol across a range of temperatures, while vacuum ultraviolet spectroscopy captured its absorption characteristics in the 115-220 nm range. Complementing these experiments, molecular dynamics simulations unravelled the microscopic interactions between the alcohol molecules, offering a new perspective on the complexity of icy mantles in space. This surprising discovery challenges conventional ideas about the phase behavior of interstellar ices and expands our understanding of the molecular diversity in space.

Meanwhile, a different kind of light emerged from the depths of the Red Rectangle Nebula—a mysterious blue luminescence (BL). This glow had puzzled scientists for decades, with its origins tied to the enigmatic interplay of polycyclic aromatic hydrocarbons. BL is characterized by

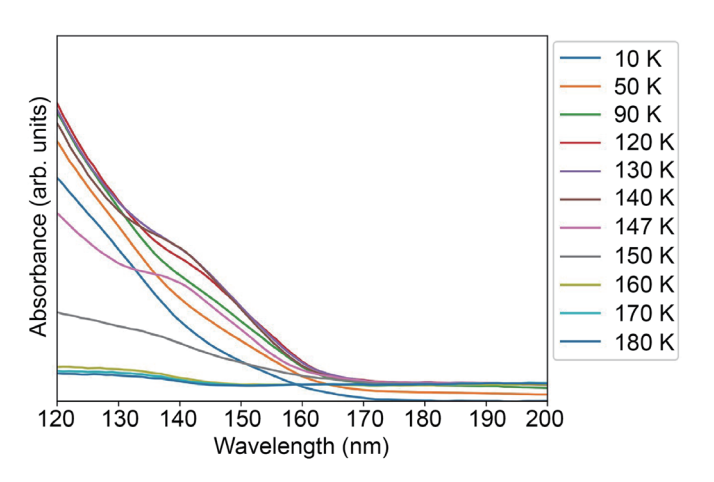


Fig. 1: VUV spectra of 1-propanol ice recorded after deposition at 10 K. The deposited ice was then warmed to higher temperatures and spectra recorded at specific temperatures until sublimation. [Reproduced from Ref. 2]

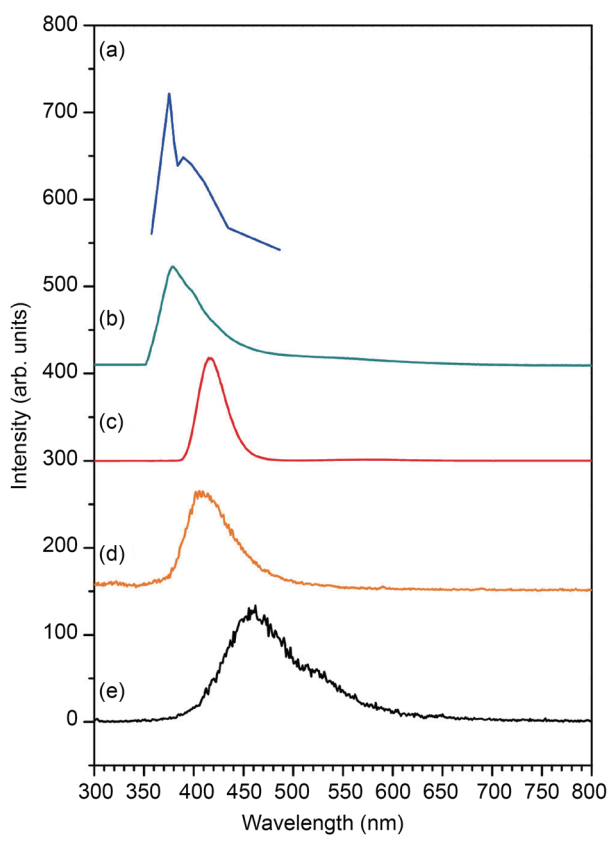


Fig. 2: (a) Blue luminescence recorded in the Red Rectangle Nebula,<sup>4</sup> and PL spectra measured at 10 K upon excitation with 121.6 nm for (b) photochemically N<sub>2</sub>-covered graphene, (c) photochemically O<sub>2</sub>-covered graphene, (d) commercial N-doped graphene flakes, and (e) commercial graphene oxide flakes. [Reproduced from Ref. 3]

an asymmetrical spectral band peaking around 375-378 nm in the ultraviolet and visible regions. Its discovery in astrophysical environments such as the Red Rectangle Nebula links it to aromatic compounds and quantum effects in interstellar dust. In a breakthrough study,3 Y.-J. Wu (NSRRC) and his collaborators turned to graphene, a material as versatile as it is remarkable. By doping graphene with nitrogen atoms and exposing it to VUV light, they recreated conditions that echoed the astrophysical environments where BL thrives. The experimental setup involved single-layer graphene films, covered by a few layers of N2 or O2 solids and mounted on MgF2 substrates, which were then cooled to 10 K and exposed to intense VUV light at 121.6 nm at TLS 21A2. Photoluminescence spectroscopy revealed a peak at 378 nm, closely matching the BL spectra recorded in the Red Rectangle Nebula, as shown in Fig. 2. Further analysis using Raman spectroscopy and X-ray photoelectron spectroscopy identified the structural defects and pyrrolic-N and pyridinic-N groups in the graphene lattice responsible for the luminescence. These defects disrupt the carbon network's symmetry, introducing localized electronic states that emit the characteristic blue light when excited. This study established N-doped graphene as a potential carrier of BL observed in astrophysical environments.

Together, these studies weave a rich tapestry of discovery, connecting laboratory experimentation with the mysteries of the universe. They remind us that the smallest molecules, whether in icy grains or luminous nebulae, hold the power to unlock profound insights into our cosmic origins. As scientists continue to explore these molecular frontiers, the stories of ethanolamine, 1-propanol, and N-doped graphene serve as beacons, guiding us toward a deeper understanding of the molecular universe and our place within it. (Reported by Yu-Jong Wu)

This report features the work of Bhalamurugan Sivaraman and his collaborators published in Astrophys. J. **975**, 181 (2024) and MNRAS **530**, 1027 (2024), and the work of Yu-Jong Wu and his collaborators published in Astrophys. J. **977**, 230 (2024).

# TLS 03A1 High-flux VUV Beamline TLS 21A2 VUV Photochemistry

- Photoabsorption, Photoluminescence
- Astrochemistry, Molecular Science

- R. Ramachandran, M. Sil, P. Gorai, J. K. Meka, P. Sundararajan, J.-I. Lo, S.-L. Chou, Y.-J. Wu, P. Janardhan, B.-M. Cheng, A. Bhardwaj, V. M. Rivilla, N. J. Mason, B. Sivaraman, A. Das, Astrophys. 975, 181 (2024).
- R. Ramachandran, A. Hazarika, S. Gupta, S. Nag, J. K. Meka, T. S. Thakur, S. Yashonath, G. Vishwakarma, S.-L. Chou, Y.-J. Wu, P. Janardhan, B. N. Rajasekhar, A. Bhardwaj, N. J. Mason, B. Sivaraman, P. K. Maiti, MNRAS 530, 1027 (2024).
- S.-Y. Lin, S.-L. Chou, T.-P. Huang, M.-Y. Lin, H.-F. Chen,
   P. J. Sarre, C.-M. Tseng, Y.-J. Wu, Astrophys. J. 977, 230 (2024).
- 4. U. P. Vijh, A. N. Witt, K. D. Gordon, Astrophys. J. Lett. **606**, L65 (2004).